ELSEVIER

Journal of Organometallic Chemistry 550 (1998) 213–220

Journal of Organo metallic Chemistry

Preparation and structures of $\{Li[C(N^tBu)_2(HN^tBu)]\}_2 \cdot (THF)$ and $\{Li_2[C(N^tBu)_3]\}_2$, containing the novel anions $[C(N^tBu)_2(HN^tBu)]^-$ and $[C(N^tBu)_3]^{2-}$ [1]

Tristram Chivers *, Masood Parvez, Gabriele Schatte

Department of Chemistry, The University of Calgary, Calgary, Alta. T2N 1N4, Canada

Received 11 February 1997

Abstract

The reaction of *tert*-butyl carbodiimide with one equivalent of $LiNH^tBu$ in tetrahydrofuran at −78 °C produces $\{Li[C(N^tBu)_2(HN^tBu)]\}_2 \cdot (THF)$ (**1**), which is an eight-membered $Li_2C_2N_4$ ring; the deprotonation of **1** with two equivalents of *n*-BuLi in tetrahydrofuran at −78 °C and recrystallization of the product from *n*-pentane yielded the unsolvated dimer $\{Li_2[C(N^tBu)_3]\}_2$ (**2**), which has a distorted cyclic ladder structure. © 1998 Elsevier Science S.A.

Keywords: Hetero-trimethylenemethane ligands; C–N–Li cluster; Carbodiimides; X-ray structure

1. Introduction

The revival of interest in the chemistry of metal complexes containing trimethylenemethane ($C(CH_2)_3^{2-}$, TMM) and, especially, heteroatom-substituted TMM ligands, is illustrated by three recent publications concerning the triazatrimethylene methane dianion $C(NPh)_3^{2-}$ [2,3]. In 1995 the preparation and structure of the tetrahydrofuran solvate $\{Li_2[C(NPh)_3](THF)_3\}_2$ was reported [2]. The synthetic method involved the deprotonation of *N,N′,N″*-triphenylguanidine with two equivalents of *n*-butyllithium. Since guanidine derivatives are not always easily accessible (e.g. the synthesis of *N,N′,N″*-tri(*tert*-butyl)guanidine requires multiple steps [4]), we have been investigating a more versatile route to hetero-trimethylenemethane ligands. Recently, we and others have shown that the novel dianions $E(N^tBu)_3^{2-}$ (E = Te [5,6], Se [7], S [8]) can be generated by the reaction of the appropriate chalcogen diimide $^tBuN{=}E{=}N^tBu$ with two molar equivalents of lithium *tert*-butylamide, $LiNH^tBu$ (Eq. (1)).

$$^tBuN{=}E{=}N^tBu + 2\,LiNH^tBu \rightarrow \tfrac{1}{2}\{Li_2[E(N^tBu)_3]\}_2 + {}^tBuNH_2 \quad (1)$$

By analogy with this synthetic approach we reasoned that commercially available carbodiimides, which are known to react readily with organolithium reagents [9], might serve as a convenient source of triazatrimethylene methane dianions (Eq. (2)).

$$RN{=}C{=}NR + 2LiNH^tBu \rightarrow Li_2[C(NR)_2(N^tBu)] + {}^tBuNH_2 \quad (2)$$

Here we report the syntheses and the single-crystal X-ray structures of $\{Li[C(N^tBu)_2(HN^tBu)]\}_2(THF)$ (**1**) and the unsolvated dimer $\{Li_2[C(N^tBu)_3]\}_2$ (**2**), which contain the novel anions $[C(N^tBu)_2(HN^tBu)]^-$ and $[C(N^tBu)_3]^{2-}$ respectively.

2. Experimental

1,3-Di-*tert*-butyl carbodiimide, $^tBuN{=}C{=}N^tBu$, (Aldrich) was used after its purity was checked by ^1H, ^{13}C FT-NMR and FT-IR spectroscopy. $LiNH^tBu$ was prepared from anhydrous $^tBuNH_2$ (Aldrich, pre-dried over KOH and then distilled from CaH_2 onto molecular

* Corresponding author.

[1] Dedicated to Professor Ken Wade on the occasion of his 65th birthday and in recognition of his many contributions to inorganic chemistry, including the 'laddering principle' in lithium amide chemistry [1].

sieves) and *n*-BuLi (Aldrich, 2.5 M solution in hexanes) in toluene [10] and recrystallized from *n*-hexane. Solvents were dried with the appropriate drying agents [11] and distilled immediately before use. All reactions and the manipulation of moisture-sensitive products were carried out under an atmosphere of argon or under vacuum. All glassware was carefully dried prior to use.

^{1}H NMR spectra were recorded on Bruker ACE 200 and AM 400 spectrometers, and chemical shifts are reported relative to Me_4Si in $CDCl_3$. ^{13}C and ^{7}Li NMR spectra were measured at 300 K in d_6-benzene or d_8-THF and in the range of 320 to 185 K in d_8-toluene on a Bruker AM 400 spectrometer using a 10 mm broadband probe operating at 100.614 MHz and 155.503 MHz respectively. The samples were externally referenced to either TMS in $CDCl_3$ or 1.0 M LiCl in D_2O respectively. Line-broadening parameters, used in the exponential multiplication of the free induction decays, were 0.5 Hz. A relaxation delay of 3 s was applied when measuring the ^{13}C NMR spectra. Infrared spectra were obtained as Nujol mulls on a Mattson 4030 FT-IR spectrometer in the range of 4000–350 cm^{-1} (resolution: 4 cm^{-1}; number of scans: 128). Elemental analyses were provided by the Analytical Services Laboratory, Department of Chemistry, The University of Calgary.

2.1. Synthesis of $\{Li[C(N^tBu)_2(HN^tBu)]\}_2(THF)$ (1)

The synthesis of $\{Li[C(N^tBu)(HN^tBu)]\}_2(THF)$ was carried out in a one-piece apparatus consisting of three thick-walled round-bottom flasks (25 ml) linked by a glass tube (o.d. 10 mm) incorporating a sintered-glass filter disc (medium porosity). The three bulbs were fitted with Pyrex glass valves with Teflon pistons (J. Young, London) (see Fig. 1). ^{t}BuN=C=N^{t}Bu (0.9996 g, 6.48 mmol) and THF (5 ml) were added to bulb (B) of the reaction vessel and the Teflon piston was replaced by a septum. A solution of LiNH^{t}Bu (0.512 g, 6.48 mmol) in THF (10 ml) was added dropwise via a cannula to the stirred colourless solution of ^{t}BuN=C=N^{t}Bu in THF cooled to −78 °C. Upon addition the colour of the ^{t}BuN=C=N^{t}Bu/THF solution changed to pale yellow. The reaction mixture was warmed slowly to 23 °C after stirring the mixture for 0.5 h at −78 °C. The volatile materials were then removed under dynamic vacuum leaving a white solid identified as $\{Li[C(N^tBu)_2(HN^tBu)]\}_2(THF)$ (1.536 g, 2.85 mmol; 88%; m.p. 94 °C (decomp.)). Anal. Calcd. for $C_{30}H_{64}Li_2N_6O$ (%): C, 66.88; H, 11.97; N, 15.60. Found: C, 65.53, H, 10.91; N, 15.12. IR (KBr, Nujol), ν (cm^{-1}): 3459 (w) [ν(NH)], (2132, 2102) [ν(N–C=N)], 1539 (s) [ν(C=N)], (1197 (s, br), 1039 (m)} [ν(C–N], 1100–1000 (vibrations due to N^{t}Bu groups), 553 cm^{-1} (characteristic for Li salts containing N^{t}Bu groups; see Ref. [7]); ^{1}H NMR (400 MHz, δ(TMS in $CDCl_3$)); in C_6D_6: 3.81 (NH), 3.58 (m) (THF), 1.48 (br) (THF), 1.41, 1.39, 1.29; in d_8-THF: 1.25 (18 H), 1.18 (36 H) at 25 °C; ^{7}Li NMR (400 MHz, δ(1 M LiCl in D_2O)); d_8-THF: $\delta = 1.76$, 0.97 at 25 °C; in C_7D_8 at 48 °C: −0.59, −1.97, −2.35 (ratio 2:1:1); ^{13}C NMR (400 MHz, d_8-THF, δ(TMS in $CDCl_3$)): $\delta = 167.9$ (s) [C(N^{t}Bu)$_2$(HN^{t}Bu)], 55.0 (s) [–N(H)C(CH$_3$)$_3$], 51.2 (m, br) [–NC(CH$_3$)$_3$], 38.7 (s), 33.7, 33.4, 31.8 (s) [−C(CH$_3$)$_3$] at 25 °C.

Crystals of $\{Li[C(N^tBu)_2(HN^tBu)]\}_2(THF)$ suitable for X-ray diffraction were obtained from the reaction of ^{t}BuN=C=N^{t}Bu (0.504 g, 3.27 mmol) in THF (5 ml) and LiNH^{t}Bu (0.517 g, 6.53 mmol) in THF (10 ml) using the three-bulbed reaction vessel (see Fig. 1). After removal of the volatile materials under vacuum, the solid obtained in flask (B) was dissolved in *n*-pentane (ca. 10 ml) under an Ar atmosphere and the solution was filtered through the frit into flask (A). The solution was degassed using the freeze–pump–thaw technique and the reaction vessel was evacuated. The solvent was slowly condensed into flask (B) under static vacuum ($\Delta T = 5$ °C) and small crystals of **1** formed in flask (A). The crystalline solid in (A) was then divided into two halves by partially dissolving the solid in *n*-pentane (ca. 5 ml) which was condensed back from (B). The solution was transferred into flask (C) and the remaining solid left in flask (A) was dissolved in *n*-pentane left behind in (B). Slow removal of the solvent from flask (A) ($T = 19$ °C) into flask (B) ($T = 14$ °C) over a period of 2.5 days resulted in the formation of a large crystal surrounded by small crystals. Block-shaped transparent crystals, which were suitable for X-ray diffraction, were also observed in the golden-yellow solution in flask (C).

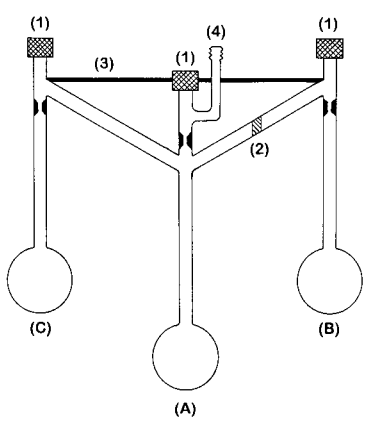

Fig. 1. Three-bulb glass reaction vessel: (A, B, C) thick-walled round bottom flasks (25 ml); (1) Teflon-stemmed Pyrex glass valves (PTT/5/RA, SPTT5; J. Young, UK); (2) sintered glass filter disk (medium); (3) supporting glass rod; (4) hose connection.

2.2. Synthesis of $\{Li_2[C(N^tBu)_3]\}_2$ (2)

A solution of *n*-BuLi (1.86 mmol) in hexanes was added dropwise to the solution of **1** (0.500 g,

0.928 mmol) in THF (ca. 10 ml) at −78 °C using Schlenk techniques. The mixture was allowed to reach 23 °C slowly, and the colour of the solution changed from pale yellow to colourless. The volatiles were removed under dynamic vacuum, giving in quantitative yield the white solid $\{Li_2[C(N^tBu)_3]\}_2(THF)$ (0.560 g, 1.02 mmol; m.p. 124–125 °C (decomp.)). According to the ^1H NMR spectrum in d_6-benzene the product contained THF. Recrystallization of the product from *n*-pentane using a two-bulb reaction vessel ($\Delta T = 5$ °C) and the technique described above for **1** produced rectangular-shaped crystals of $\{Li_2[C(N^tBu)_3]\}_2$ (**2**) (m.p. 134 °C (decomp.)) after 1 day. Anal. Calcd. for $C_{13}H_{27}Li_2N_3$: C, 65.26; H, 11.37; N, 17.56. Found: C, 63.22, H, 10.41; N, 16.16. IR (KBr, Nujol), ν (cm^{-1}): (2132, 2102) [ν(N=C=N)], 1545 (m) [ν(C–N)], 1329 (s) [ν(C–N], [1208 (m), 1180 (s)] (vibrations due to N^tBu groups), 567 cm^{-1} (characteristic for Li salts containing N^tBu groups). ^1H NMR (400 MHz, δ(TMS in $CDCl_3$)); in C_6D_6: (3.53, 1.58, 1.52) [THF], 1.40 [^tBu]; in d_8-THF: 1.27 [^tBu] at 25 °C; ^7Li NMR (400 MHz, δ(1 M LiCl in D_2O)); in C_6D_6: −2.37, −2.52; in d_8-THF: 0.95, 0.23 at 25 °C; ^{13}C NMR (400 MHz, C_6D_6 and d_8-THF, δ(TMS in $CDCl_3$)): $\delta = 181.7$ (s) [$C(N^tBu)_3$], 52.1 [$-C(CH_3)_3$], 34.3 (s) [$-C(CH_3)_3$] at 25 °C.

2.3. Crystal structures of 1 and 2

Crystals of **1** (colourless, prismatic) and **2** (colourless plates) were examined in a dry-box under a Wild M3 microscope mounted outside the dry-box. A single crystal was then mounted directly from the *n*-pentane solution on a glass fibre coated with epoxy (**1**) or sealed in a glass capillary tube (i.d. 1.0 mm) (**2**). The data for **1** and **2** were collected on a Rigaku AFC6S diffractometer with graphite-monochromated Mo Kα radiation at −103 ± 1 °C using ω–2θ scans ($2\theta_{max} = 50.1°$).

Crystal data for **1**: $C_{30}H_{64}N_6Li_2O$, $M = 538.75$; crystal dimensions: 0.75 × 0.55 × 0.50 mm^3; monoclinic, space group $P2_1/n$ (No. 14); $a = 20.852(5)$ Å, $b = 18.198(3)$ Å, $c = 20.988(3)$ Å, $\beta = 114.94(1)°$, $V = 7221(2)$ Å^3, $Z = 8$, $D_c = 0.991$ g cm^{-3}, $F(000) = 2400$, μ(Mo Kα) = 0.60 cm^{-1}, λ(Mo Kα) = 0.71069 Å. Of the 11 844 reflections collected 11 459 were unique ($R_{int} = 0.0584$). The intensities of three representative reflections were measured after every 500 reflections. Over the course of data collection the standards decreased by 17%. A linear correction factor was applied to the data to account for this phenomenon. The final R and R_w values were 0.070 and 0.086 respectively for 3346 observed reflections ($I > 3\sigma(I)$) and 704 parameters. The structure was determined by direct methods (SIR92) [12] and expanded using Fourier techniques (DIRDIF 94) [13]. The data were corrected for Lorentz and polarization effects. An empirical correction using ψ scans was applied, which resulted in absorption coefficients ranging from 0.62 to 1.00. A correction for secondary extinction was applied (coefficient: 0.92730 × 10^{-9}). Refinement was by full-matrix least squares, with all non-hydrogen atoms assigned anisotropic thermal parameters. Hydrogen atoms were included at geometrically idealized positions with C–H and N–H 0.95 Å. The hydrogen atoms attached to the nitrogen atoms were located from a Fourier difference map. Scattering factors were taken from Ref. [14] and effects of anomalous dispersion were included in F_c using the values given in Ref. [15].

Crystal data for **2**: $C_{26}H_{54}N_6Li_4$, $M = 478.52$; crystal dimensions: 0.80 × 0.45 × 0.30 mm^3; triclinic, space group $P\bar{1}$ (No. 2); $a = 16.794(5)$ Å, $b = 16.918(5)$ Å, $c = 9.358(2)$ Å, $\alpha = 95.30(2)°$, $\beta = 93.31(2)°$, $\gamma = 60.99(2)°$, $V = 2314(1)$ Å^3, $Z = 3$, $D_c = 1.03$ g cm^{-3}, $F(000) = 792$, μ(Mo Kα) = 0.60 cm^{-1}, λ(Mo Kα) = 0.71069 Å. Of the 8923 reflections collected, 8186 were unique ($R_{int} = 0.055$). The intensities of three representative reflections were measured after every 500 reflections. Over the course of data collection the standards decreased by 11.2%. A linear correction factor was applied to the data to account for this phenomenon. The final R and R_w values were 0.065 and 0.058 respectively for 2960 observed reflections ($I > 3\sigma(I)$) and 487 parameters. The structure was obtained by direct methods (SAPI 91) [16] and expanded using Fourier techniques (DIRDIF 94) [13]. Data correction and refinement of the structure followed the same procedures as described above for **1**. No correction for secondary extinction was applied. The empirical correction using ψ-scans led to absorption coefficients ranging from 0.97 to 1.00.

All calculations were performed by using the program TEXSAN [17]. Tables of hydrogen atomic coordinates, anisotropic thermal parameters, and a complete listing of bond lengths and angles for **1** and **2** have been deposited at the Cambridge Crystallographic Data Centre.

3. Results and discussion

$\{Li[C(N^tBu)_2(HN^tBu)]\}_2(THF)$ (**1**) was obtained in 88% yield by the reaction of 1,3-di-*tert*-butyl carbodiimide with $LiNH^tBu$ in a molar ratio of 1:1 in THF (Eq. (3)).

$$2^tBuN{=}C{=}N^tBu + 2LiNH^tBu \xrightarrow{THF} \underset{(1)}{\{Li[C(N^tBu)_2(HN^tBu)]\}_2(THF)} \quad (3)$$

The complex **1** is also the exclusive product when an excess of $LiNH^tBu$ is used. Apparently, $LiNH^tBu$ is not a sufficiently strong base to deprotonate **1**. For comparison we note that the analogous tellurium species

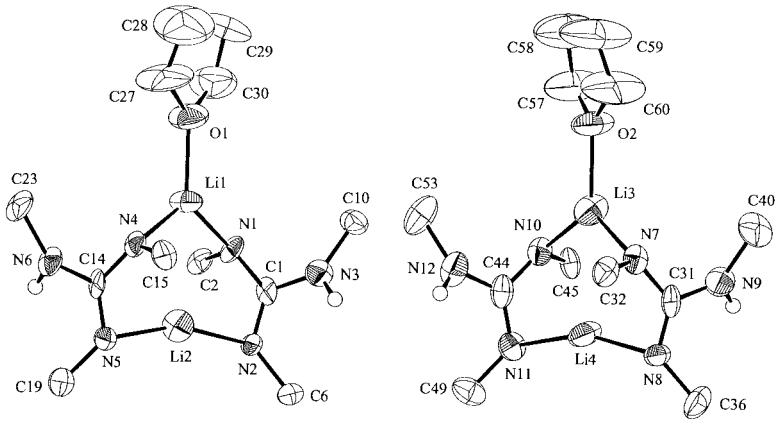

Fig. 2. Crystal structure of $\{Li[C(N^tBu)_2(HN^tBu)]\}_2(THF)$ (**1**) (both conformers). For clarity only the α-carbon atoms of the ^{t}Bu are shown. The thermal ellipsoids are scaled to enclose 50% of the probability density (ORTEP, included in the TEXSAN program package [17]).

$[Te(N^tBu)_2(HN^tBu)]^-$ is formed in the reaction of *tert*-butyl tellurium diimide with $LiNH^tBu$, but this monoanion is readily deprotonated by $LiNH^tBu$ [18]. However, the reaction of **1** with two molar equivalents of *n*-BuLi affords $\{Li_2[C(N^tBu)_3]\}_2(THF)$ (**2 · THF**) in quantitative yield (Eq. (4)). Recrystallization from *n*-pentane yielded the unsolvated dimer $\{Li_2[C(N^tBu)_3]\}_2$ (**2**), containing the novel dianion $[C(N^tBu)_3]^{2-}$.

$$\{Li[C(N^tBu)_2(HN^tBu)]\}_2(THF) + 2\,n\text{-BuLi} \xrightarrow{\text{THF–hexanes}} \{Li_2[C(N^tBu)_3]\}_2(THF) + 2\,n\text{-BuH} \quad (4)$$

X-ray diffraction studies were carried out on the compounds **1** and **2**, the structures of which are shown in Figs. 2 and 3 respectively. Tables 1 and 2 give the atomic coordinates for **1** and **2**, respectively; the values of selected bond lengths and angles are listed in Tables 3 and 4 for **1** and **2**, respectively.

The crystal structure of **1** consists of two independent eight-membered $Li_2N_4C_2$ rings with twisted chair conformations, in which two $[C(N^tBu)_2(HN^tBu)]^-$ ions are bridged by two lithium atoms (see Fig. 2). The CN bond distances of 1.32(1) Å and of 1.37(1) Å in the $Li_2N_4C_2$ ring suggest a tendency toward CN double and CN single bonds respectively (cf. mean values of 1.36 Å for $C(sp^2)$–N and 1.29 Å for $C(sp^2)$=N [19]) and limited delocalization of negative charge (cf. (**3**)). The exocyclic CN bond lengths of 1.39(1) Å are consistent with a $C(sp^2)$–N single bond and the presence of a hydrogen atom on the exocyclic nitrogen. The sum of the bond angles at the central carbon atoms C(14)/C(1) and C(44)/C(31) is close to 360°.

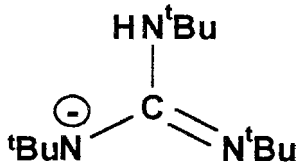

(3)

Both two- and three-coordinate lithium ions are observed in this structure, with mean Li–N lengths of 1.97(2) Å (Li(4)/Li(2); coordinated to two nitrogen atoms) and 2.03(2) Å (Li(3)/Li(1); coordinated to two

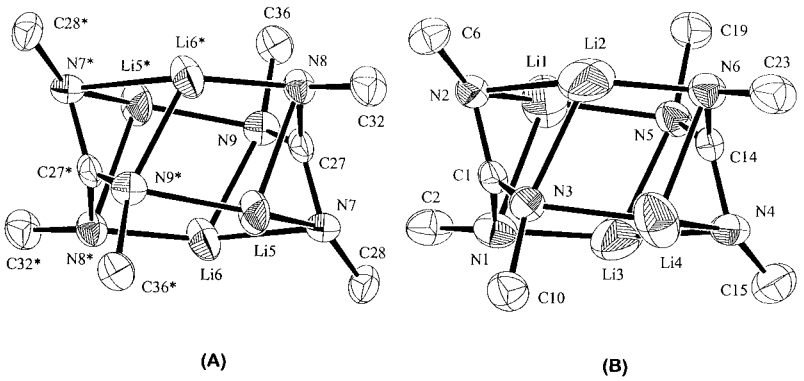

Fig. 3. ORTEP diagram (50% probability ellipsoids) and atomic numbering for $\{Li_2[C(N^tBu)_3]\}_2$ (**2**): (**A**) centrosymmetric $C_2N_6Li_4$ cage; (**B**) second $C_2N_6Li_4$ cage. For clarity only the α-carbon atoms of the ^{t}Bu are shown. The thermal ellipsoids are scaled to enclose 50% of the probability density (ORTEP, included in the TEXSAN program package [17]). Starred atoms are related to the unstarred atoms by $-x-1$, $-y+1$, $-z+1$.

Table 1
Atomic coordinates and thermal parameters for non-hydrogen atoms in **1**

Atom	x	y	z	B_{eq} [a]
O(1)	0.1389(4)	0.4292(4)	0.2987(4)	6.2(2)
O(2)	0.1748(4)	0.3887(4)	0.8386(4)	6.4(2)
N(1)	0.0390(4)	0.2849(4)	0.1928(3)	2.8(2)
N(2)	0.0417(4)	0.1745(4)	0.1366(3)	2.8(2)
N(3)	0.0512(4)	0.2883(4)	0.0869(4)	3.6(2)
N(4)	0.2055(4)	0.2482(4)	0.3197(3)	2.7(2)
N(5)	0.1869(4)	0.1206(4)	0.3188(3)	3.1(2)
N(6)	0.1813(4)	0.1950(4)	0.4080(4)	3.3(2)
N(7)	0.1904(4)	0.1991(4)	0.8072(3)	3.1(2)
N(8)	0.2177(4)	0.0797(4)	0.8542(4)	3.1(2)
N(9)	0.1128(5)	0.1386(4)	0.8436(4)	4.2(2)
N(10)	0.3062(4)	0.2772(4)	0.9637(4)	3.2(2)
N(11)	0.3850(4)	0.1782(5)	0.9854(4)	3.7(2)
N(12)	0.4059(4)	0.2922(5)	0.9430(4)	4.4(2)
C(1)	0.0417(4)	0.2468(6)	0.1388(5)	2.6(2)
C(2)	−0.0132(5)	0.2597(5)	0.2199(4)	2.9(3)
C(3)	−0.0192(5)	0.3215(6)	0.2638(5)	5.4(3)
C(4)	0.0076(5)	0.1901(5)	0.2659(4)	3.7(3)
C(5)	−0.0864(5)	0.2469(6)	0.1601(4)	4.3(3)
C(6)	0.0277(5)	0.1284(5)	0.0740(5)	3.2(3)
C(7)	0.0886(6)	0.1255(6)	0.0516(5)	5.2(3)
C(8)	−0.0411(5)	0.1493(6)	0.0094(5)	5.6(3)
C(9)	0.0177(6)	0.0511(6)	0.0964(5)	6.1(4)
C(10)	0.0346(5)	0.3651(5)	0.0641(5)	3.5(3)
C(11)	−0.0342(6)	0.3900(6)	0.0644(6)	6.2(4)
C(12)	0.0302(6)	0.3696(6)	−0.0106(5)	6.2(4)
C(13)	0.0933(6)	0.4143(6)	0.1116(6)	6.2(4)
C(14)	0.1938(5)	0.1852(6)	0.3484(4)	3.0(3)
C(15)	0.2566(5)	0.2438(5)	0.2879(5)	3.7(3)
C(16)	0.2289(5)	0.2087(6)	0.2148(5)	5.2(3)
C(17)	0.2783(5)	0.3224(6)	0.2817(6)	5.7(3)
C(18)	0.3243(5)	0.2021(6)	0.3351(5)	4.8(3)
C(19)	0.1899(6)	0.0497(6)	0.3532(5)	4.4(3)
C(20)	0.1997(6)	−0.0066(6)	0.3058(6)	6.5(4)
C(21)	0.1220(7)	0.0300(6)	0.3612(6)	6.8(4)
C(22)	0.2543(6)	0.0433(5)	0.4261(5)	6.2(3)
C(23)	0.2065(6)	0.2510(6)	0.4649(5)	4.0(3)
C(24)	0.2058(7)	0.2143(7)	0.5303(5)	7.8(4)
C(25)	0.2806(6)	0.2776(6)	0.4800(5)	5.8(3)
C(26)	0.1575(6)	0.3155(7)	0.4444(5)	6.6(3)
C(27)	0.2031(8)	0.4655(8)	0.3456(8)	10.9(5)
C(28)	0.1916(11)	0.5386(11)	0.3417(11)	14.1(8)
C(29)	0.1215(12)	0.5544(7)	0.2868(10)	11.0(6)
C(30)	0.0837(7)	0.4824(8)	0.2780(7)	8.4(5)
C(31)	0.1745(6)	0.1362(6)	0.8335(5)	3.2(3)
C(32)	0.2241(5)	0.1905(5)	0.7587(5)	3.5(3)
C(33)	0.2178(6)	0.2645(6)	0.7228(5)	5.6(3)
C(34)	0.3019(6)	0.1701(6)	0.7905(5)	5.7(3)
C(35)	0.1852(5)	0.1336(6)	0.6997(5)	5.7(3)
C(36)	0.1980(6)	0.0050(6)	0.8663(5)	4.5(3)
C(37)	0.1298(6)	−0.0238(6)	0.8071(6)	6.3(3)
C(38)	0.2588(7)	−0.0433(6)	0.8684(7)	8.3(5)
C(39)	0.1934(6)	−0.0032(6)	0.9370(6)	6.2(3)
C(40)	0.0457(6)	0.1793(7)	0.8050(5)	4.9(3)
C(41)	−0.0102(6)	0.1383(7)	0.8193(6)	8.3(4)
C(42)	0.0258(6)	0.1806(11)	0.7288(6)	13.4(6)
C(43)	0.0520(8)	0.2564(8)	0.8351(10)	12.1(6)
C(44)	0.3670(6)	0.2471(6)	0.9667(5)	3.4(3)
C(45)	0.2848(5)	0.2583(5)	1.0207(4)	2.9(2)
C(46)	0.2292(6)	0.3143(6)	1.0167(5)	5.6(3)
C(47)	0.2521(5)	0.1825(5)	1.0149(4)	4.3(3)
C(48)	0.3468(5)	0.2653(6)	1.0936(5)	5.4(3)
C(49)	0.4563(6)	0.1467(6)	1.0088(5)	4.2(3)
C(50)	0.4729(5)	0.1268(6)	0.9465(6)	6.0(3)
C(51)	0.4536(6)	0.0760(7)	1.0442(7)	8.0(4)
C(52)	0.5157(6)	0.1954(7)	1.0620(6)	7.5(4)
C(53)	0.4162(7)	0.3728(6)	0.9441(6)	5.3(4)
C(54)	0.4133(8)	0.4089(6)	1.0062(7)	9.2(5)
C(55)	0.4868(7)	0.3872(7)	0.9406(7)	8.8(5)
C(56)	0.3582(8)	0.4039(7)	0.8758(8)	10.0(5)
C(57)	0.1816(8)	0.4505(8)	0.8832(7)	9.6(5)
C(58)	0.1582(10)	0.5142(9)	0.8390(10)	12.6(6)
C(59)	0.1213(11)	0.4859(10)	0.7667(10)	14.0(7)
C(60)	0.1285(8)	0.4120(9)	0.7692(6)	11.3(5)
Li(1)	0.1285(9)	0.3232(9)	0.2701(8)	3.9(4)
Li(2)	0.1162(9)	0.1670(9)	0.2339(8)	4.3(5)
Li(3)	0.2213(9)	0.2890(9)	0.8677(8)	4.9(5)
Li(4)	0.2928(9)	0.1485(8)	0.9142(8)	4.5(5)

[a] $B_{eq} = (8/3\ \pi^2[U_{11}(aa^*)^2 + U_{22}(bb^*)^2 + U_{33}(cc^*)^2 + 2U_{12}aa^*bb^*\cos\gamma + 2U_{13}aa^*cc^*\cos\beta + 2U_{23}bb^*cc^*\cos\alpha]$.

nitrogen atoms and one THF molecule) respectively. The bond distances, bond angles and the magnitude of the torsion angles (opposite in sign) in the two conformers are identical, since they are mirror images of each other (see Table 3). In contrast to the structure of the lithium *N,N′*-bis(trimethylsilyl)benzamidinate, $\{Li[C(NSiMe_3)_2(4\text{-}MeC_6H_4)]\}_2(THF)$ [20], transannular LiN bonds (e.g. Li(4)–N(10), Li(3)–N(8)) are not present in **1**. Consequently, **1** does not show the ladder-shaped arrangement which is a common structural feature in organolithium nitrogen compounds [10,21,22].

The results of a variable-temperature ^1H and ^7Li NMR of **1** in C_7D_8 in the range 185–320 K suggest the presence of more than one species in solution. The ^1H NMR spectrum at 298 K exhibited three resonances at 1.38, 1.34 and 1.29 ppm for the ^tBu groups in addition to the signals for the coordinated THF molecule and the NH group (3.81 ppm). At 200 K six resonances of approximately equal intensity are observed in the region δ 1.5–1.27 for the ^tBu groups. At this temperature two resonances for the protons of the NH groups (δ 3.86 and 3.44) and the THF molecules (δ 3.57/3.44 and 1.61/1.58) are also apparent. The ^7Li NMR spectrum showed three resonances at −0.59, −0.97 and −2.35 ppm, with approximate intensities 2:1:1, throughout the temperature range of 267 to 320 K. At temperatures below 267 K the two resonances at −0.97 and −2.35 ppm collapsed into one broad signal at

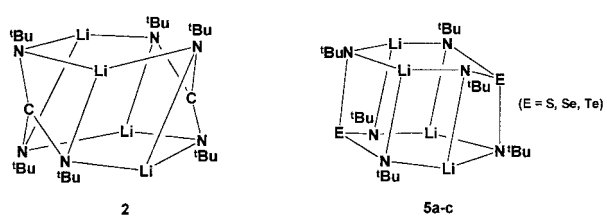

Fig. 4. Structural comparison of $\{Li_2[C(N^tBu)_3]\}_2$ (**2**) and $\{Li_2[E(N^tBu)_3]\}_2$ (E = S, Se, Te; **5a–c**).

Table 2
Atomic coordinates and thermal parameters for non-hydrogen atoms in **2**

Atom	x	y	z	B_{eq} [a]
N(1)	0.1890(3)	0.2236(4)	−0.0469(5)	2.9(1)
N(2)	0.1532(3)	0.2824(3)	0.1925(5)	2.4(1)
N(3)	0.0578(3)	0.2353(3)	0.0564(5)	2.5(1)
N(4)	0.2160(4)	−0.0013(4)	0.0197(5)	2.9(1)
N(5)	0.3117(3)	0.0469(3)	0.1529(5)	2.7(1)
N(6)	0.1814(4)	0.0572(3)	0.2583(5)	2.8(2)
N(7)	−0.3424(3)	0.4209(3)	0.5035(5)	2.1(1)
N(8)	−0.4372(3)	0.5375(3)	0.6734(5)	2.3(1)
N(9)	−0.4416(3)	0.5670(3)	0.4262(5)	2.2(1)
C(1)	0.1298(4)	0.2528(4)	0.0643(7)	2.3(2)
C(2)	0.2406(5)	0.2708(5)	−0.0820(7)	3.3(2)
C(3)	0.1851(5)	0.3742(5)	−0.0630(8)	5.4(3)
C(4)	0.2648(6)	0.2410(6)	−0.2409(8)	6.7(3)
C(5)	0.3300(5)	0.2423(5)	0.0011(8)	4.9(2)
C(6)	0.0863(4)	0.3511(4)	0.2966(7)	2.8(2)
C(7)	0.1392(5)	0.3908(5)	0.3847(7)	4.6(2)
C(8)	0.0479(5)	0.3138(5)	0.4012(7)	4.6(2)
C(9)	0.0056(5)	0.4280(5)	0.2232(7)	4.4(2)
C(10)	0.0003(5)	0.2512(5)	−0.0768(7)	3.3(2)
C(11)	0.0389(5)	0.1710(5)	−0.1942(8)	6.1(3)
C(12)	−0.0182(5)	0.3351(5)	−0.1492(7)	4.6(2)
C(13)	−0.0897(5)	0.2607(6)	−0.0306(8)	6.0(3)
C(14)	0.2400(4)	0.0282(4)	0.1487(7)	2.4(2)
C(15)	0.2835(5)	−0.0713(5)	−0.0828(8)	3.9(2)
C(16)	0.3623(6)	−0.1492(5)	−0.0098(8)	7.0(3)
C(17)	0.3234(6)	−0.0343(6)	−0.1858(8)	6.6(3)
C(18)	0.2294(6)	−0.1081(5)	−0.1754(8)	5.9(3)
C(19)	0.3692(5)	0.0329(5)	0.2864(7)	3.2(2)
C(20)	0.3334(5)	0.1140(5)	0.3980(8)	5.8(2)
C(21)	0.3846(5)	−0.0474(5)	0.3635(8)	6.0(2)
C(22)	0.4590(5)	0.0167(8)	0.2359(8)	9.5(3)
C(23)	0.1307(5)	0.0097(5)	0.2930(7)	3.9(2)
C(24)	0.1883(6)	−0.0944(6)	0.2781(9)	6.7(3)
C(25)	0.1044(6)	0.0410(6)	0.4501(8)	7.5(3)
C(26)	0.0434(5)	0.0340(6)	0.2075(8)	5.7(3)
C(27)	−0.4017(4)	0.5106(4)	0.5364(6)	2.1(2)
C(28)	−0.2706(4)	0.3882(4)	0.3950(6)	2.7(2)
C(29)	−0.1977(5)	0.2956(5)	0.4411(7)	4.1(2)
C(30)	−0.2284(5)	0.4483(5)	0.3862(7)	4.5(2)
C(31)	−0.3016(4)	0.3713(5)	0.2407(7)	4.1(2)
C(32)	−0.3769(5)	0.5000(5)	0.8011(6)	3.0(2)
C(33)	−0.2847(5)	0.4971(5)	0.7919(7)	3.9(2)
C(34)	−0.3589(5)	0.4063(5)	0.8373(6)	4.0(2)
C(35)	−0.4289(5)	0.5683(5)	0.9249(6)	4.6(2)
C(36)	−0.4657(4)	0.6647(4)	0.4477(7)	2.8(2)
C(37)	−0.3970(5)	0.6807(5)	0.5423(8)	4.8(2)
C(38)	−0.4632(5)	0.6931(5)	0.2985(7)	4.8(2)
C(39)	−0.5594(5)	0.7279(5)	0.5120(8)	4.7(2)
Li(1)	0.2717(9)	0.1813(9)	0.1559(14)	5.3(4)
Li(2)	0.1184(12)	0.1886(11)	0.2616(13)	7.3(5)
Li(3)	0.2542(11)	0.0912(10)	−0.0441(13)	6.3(5)
Li(4)	0.0987(9)	0.1003(9)	0.0555(14)	5.0(4)
Li(5)	−0.4246(7)	0.3998(8)	0.6084(12)	3.3(3)
Li(6)	−0.4464(8)	0.4547(8)	0.3346(11)	3.3(3)

[a] $B_{eq} = (8/3)\pi^2[U_{11}(aa^*)^2 + U_{22}(bb^*)^2 + U_{33}(cc^*)^2 + 2U_{12}aa^*bb^*\cos\gamma + 2U_{13}aa^*cc^*\cos\beta + 2U_{23}bb^*cc^*\cos\alpha]$.

δ −2.49. In the coordinating solvent d_8-THF the ^{1}H NMR spectrum of **1** shows only two singlets at δ 1.25 and 1.18, with relative intensities 1:2, suggesting that both Li ions are coordinated to THF. However, the ^{7}Li NMR spectrum in the same solvent exhibits two broad singlets at δ 1.76 and 0.97.

In d_8-THF at 300 K the central carbon of the $[C(HN^tBu)(N^tBu)_2]$ unit in **1** gives rise to a resonance at $\delta(^{13}C) = 167.9$, which is to considerably higher frequency than that in $^tBuN{=}C{=}N^tBu$ ($\delta(^{13}C$ in d_8-THF) 139.6 $[C(N^tBu)_2]$, 55.1 $[{=}NC(CH_3)_3]$, 31.9 $[{=}NC(CH_3)_3]$ [23]). By comparison with the ^{13}C chemical shift observed for the central carbon in $LiNH^tBu$ ($\delta(^{13}C$ in d_8-THF) 51.6 $[{-}NC(CH_3)_3]$, 38.8 $[{-}NC(CH_3)_3]$ [23]) the resonance at δ 55.0 can be assigned to the tertiary carbon of the HN^tBu fragment in **1**.

The identity of **2** was established by X-ray crystallography, which revealed a dimeric structure $\{Li_2[C(N^tBu)_3]\}_2$. The unit cell consists of two independent $C_2N_6Li_4$ cages (**A** and **B**), one of which is centrosymmetric (**A**, Fig. 3). Each $C_2N_6Li_4$ cage contains two essentially planar $C(N^tBu)_3^{2-}$ dianions ($\Sigma[\angle(C)] \approx$ 358–359°), with approximately equal (NCN) bond angles, linked by four Li atoms. By contrast, the (NCN) bond angles in $\{Li_2[C(NPh)_3]\}_2(THF)_6$ span the range 111.8(3)–126.6(3)° [2]. The mean C–N distance of 1.379(7) Å, which is comparable to the corresponding value of 1.36(1) Å found for $\{Li_2[C(NPh)_3]\}_2(THF)_6$ [2], is consistent with the resonance hybrid (**4**).

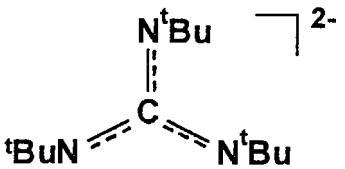

(4)

The formation of **2** from **1** can be viewed as an intramolecular process. The replacement of the hydrogen atoms attached to the exocylic nitrogen atoms by lithium results in the formation of two $\overline{CNLiNLiN}$ hexagons (e.g. N(12)–Li–N(8) and N(9)–Li–N(11) in Fig. 2). The two hexagons are then linked via LiN bonds with Li–N distances in the range 1.891(12)–2.262(12) Å, leading to the distorted cyclic ladder structure of **2**. Alternatively, the structure of **2** can be viewed as a highly distorted hexagonal prism. This cluster arrangement is clearly related to those found in **5a–c** (see Fig. 4) in which the lone pair at the chalcogen enforces a pyramidal structure for the $[E(N^tBu)_3]^{2-}$ ions (E = S, Se, Te) and the longer E–N bonds (especially for E = Se, Te) result in a more regular cyclic ladder arrangement of four-membered rings. The structure of **2** can also be correlated to the acyclic ladder-shaped structure of $\{Li_2[C(NPh)_3]\}_2(THF)_6$. As illustrated in Fig. 5, the coordination of THF molecules to

Table 3
Selected bond distance (Å) and bond angles (deg) in **1**

O(1)–Li(1)	2.00(2)	O(2)–Li(3)	2.03(2)
N(1)–C(1)	1.35(1)	N(1)–C(2)	1.50(1)
N(1)–Li(1)	2.01(2)	N(2)–C(1)	1.32(1)
N(2)–O(6)	1.48(1)	N(2)–Li(2)	1.98(2)
N(3)–C(1)	1.41(1)	N(3)–C(10)	1.47(1)
N(4)–C(14)	1.36(1)	N(4)–C(15)	1.48(1)
N(4)–Li(1)	2.03(2)	N(5)–C(14)	1.31(1)
N(5)–C(19)	1.47(1)	N(2)–Li(2)	1.96(2)
N(6)–C(14)	1.39(1)	N(6)–O(23)	1.49(1)
N(7)–C(31)	1.37(1)	N(7)–C(32)	1.47(1)
N(7)–Li(3)	2.00(2)	N(8)–C(31)	1.32(1)
N(8)–C(36)	1.47(1)	N(8)–Li(4)	1.99(2)
N(9)–C(31)	1.39(1)	N(9)–C(40)	1.48(1)
N(10)–C(44)	1.36(1)	N(10)–C(45)	1.48(1)
N(10)–Li(3)	2.06(2)	N(11)–C(44)	1.32(1)
N(11)–C(49)	1.47(1)	N(11)–Li(4)	1.95(2)
N(12)–C(44)	1.39(1)	N(12)–C(53)	1.48(1)
C(27)–O(1)–C(30)	107.1(9)	C(27)–O(1)–Li(1)	126.7(9)
C(30)–O(1)–Li(1)	126.2(9)	C(57)–O(2)–O(60)	105.8(9)
C(57)–O(2)–Li(3)	127.1(8)	C(60)–O(2)–Li(3)	127.1(9)
C(1)–N(1)–O(2)	117.2(7)	C(1)–N(1)–Li(1)	120.2(7)
C(2)–N(1)–Li(1)	112.0(7)	C(1)–N(2)–O(6)	126.5(7)
C(1)–N(2)–Li(2)	92.5(7)	C(6)–N(2)–Li(2)	130.6(8)
C(1)–N(2)–C(10)	132.2(8)	C(14)–N(4)–C(15)	116.8(8)
C(14)–N(4)–Li(1)	122.8(7)	C(15)–N(4)–Li(1)	111.7(7)
C(14)–N(5)–C(19)	125.6(7)	C(14)–N(5)–Li(2)	86.3(7)
C(19)–N(5)–Li(2)	133.3(8)	C(14)–N(6)–C(23)	132.3(8)
C(31)–N(7)–C(32)	117.3(8)	C(31)–N(7)–Li(3)	119.6(7)
C(32)–N(7)–Li(3)	114.0(8)	C(31)–N(8)–C(36)	125.2(9)
C(31)–N(8)–Li(4)	87.9(7)	C(36)–N(8)–Li(4)	132.5(8)
C(31)–N(9)–C(40)	130.7(8)	C(44)–N(10)–C(45)	117.5(8)
C(44)–N(10)–Li(3)	119.3(8)	C(45)–N(10)–Li(3)	112.8(8)
C(44)–N(11)–Li(49)	126.2(9)	C(44)–N(11)–Li(4)	88.3(7)
C(49)–N(11)–Li(4)	132.7(8)	C(44)–N(12)–C(53)	133.1(9)
N(1)–C(1)–N(2)	123.0(8)	N(1)–C(1)–N(3)	116.4(8)
N(2)–C(1)–N(3)	120.4(8)	N(1)–C(2)–C(3)	105.6(8)
N(1)–C(2)–C(4)	115.7(7)	N(1)–C(2)–C(5)	111.6(7)
N(4)–C(14)–N(5)	123.2(8)	N(4)–C(14)–N(6)	115.2(9)
N(5)–C(14)–N(6)	121.2(9)	N(7)–C(31)–N(8)	122.5(10)
N(7)–C(31)–N(9)	115.6(10)	N(8)–C(31)–N(9)	121.6(10)
N(10)–C(44)–N(11)	122.6(10)	N(10)–C(44)–N(12)	114(1)
N(11)–C(44)–N(12)	122(1)	O(1)–Li(1)–N(1)	121.4(9)
O(1)–Li(1)–N(4)	122.1(8)	N(1)–Li(1)–N(4)	116.4(8)
N(2)–Li(2)–N(5)	158(1)	O(2)–Li(3)–N(7)	123.8(8)
O(2)–Li(3)–N(10)	119.6(9)	N(7)–Li(3)–N(10)	116.7(9)
N(8)–Li(4)–N(11)	157.0(10)		
N(1)–Li(1)–O(1)–C(30)	11(1)		
N(1)–Li(1)–N(4)–C(15)	93.6(10)		
N(4)–Li(1)–O(1)–C(30)	−165(1)		
N(4)–Li(1)–N(1)–C(2)	88.4(9)		
N(4)–Li(1)–O(1)–C(27)	12(1)		
N(7)–Li(3)–O(2)–C(57)	164(1)		
N(7)–Li(3)–O(2)–C(60)	−16(1)		
N(7)–Li(3)–N(10)–C(45)	−91(1)		
N(10)–Li(3)–O(2)–C(57)	−16(1)		
N(10)–Li(3)–O(2)–C(60)	162(1)		
N(10)–Li(3)–N(7)–C(32)	−91(1)		

Table 4
Selected bond distance (Å) and bond angles (deg) in **2**[a]

N(1)–C(1)	1.365(7)	N(1)–C(2)	1.499(8)
N(1)–Li(1)	2.243(13)	N(1)–Li(3)	1.962(15)
N(2)–C(1)	1.368(7)	N(2)–C(6)	1.487(7)
N(2)–Li(1)	1.917(14)	N(2)–Li(2)	2.101(15)
N(3)–C(1)	1.373(7)	N(3)–C(10)	1.493(7)
N(3)–Li(2)	2.150(15)	N(3)–Li(4)	2.041(14)
N(4)–C(14)	1.377(7)	N(4)–C(15)	1.490(8)
N(4)–Li(3)	2.099(15)	N(4)–Li(4)	1.906(14)
N(5)–C(14)	1.383(8)	N(5)–C(19)	1.497(7)
N(5)–Li(1)	2.032(14)	N(5)–Li(3)	2.059(14)
N(6)–C(14)	1.349(7)	N(6)–C(23)	1.490(8)
N(6)–Li(2)	1.942(16)	N(6)–Li(4)	2.243(13)
N(7)–C(27)	1.368(7)	N(7)–C(28)	1.477(7)
N(7)–Li(5)	1.922(11)	N(7)–Li(6)	2.181(12)
N(8)–C(27)	1.388(7)	N(8)–C(32)	1.494(7)
N(8)–Li(5)	2.262(12)	N(8)–Li(6)*	1.891(12)
N(9)–C(27)	1.380(7)	N(9)–C(36)	1.495(7)
N(9)–Li(5)*	2.049(11)	N(9)–Li(6)	2.047(12)
C(1)–N(1)–C(2)	123.2(6)	C(1)–N(1)–Li(1)	72.4(5)
C(1)–N(1)–Li(3)	104.6(6)	C(2)–N(1)–Li(1)	89.8(5)
C(2)–N(1)–Li(3)	118.8(6)	Li(1)–N(1)–Li(3)	69.2(6)
C(1)–N(2)–C(6)	124.1(5)	C(1)–N(2)–Li(1)	84.5(5)
C(1)–N(2)–Li(2)	79.5(5)	C(6)–N(2)–Li(1)	149.1(6)
C(6)–N(2)–Li(2)	87.7(6)	Li(1)–N(2)–Li(2)	86.4(6)
C(1)–N(3)–C(10)	120.5(5)	C(1)–N(3)–Li(2)	77.6(5)
C(1)–N(3)–Li(4)	112.5(6)	C(10)–N(3)–Li(2)	161.4(6)
C(10)–N(3)–Li(4)	96.0(5)	Li(2)–N(3)–Li(4)	71.0(6)
C(14)–N(4)–C(15)	123.4(6)	C(14)–N(4)–Li(3)	78.0(5)
C(14)–N(4)–Li(4)	84.5(5)	C(15)–N(4)–Li(3)	8.84(5)
C(15)–N(4)–Li(4)	149.8(6)	Li(3)–N(4)–Li(4)	86.7(6)
C(14)–N(5)–C(19)	119.6(5)	C(14)–N(5)–Li(1)	113.6(6)
C(14)–N(5)–Li(3)	79.3(5)	C(19)–N(5)–Li(1)	94.3(5)
C(19)–N(5)–Li(3)	160.4(6)	Li(1)–N(5)–Li(3)	71.8(5)
C(14)–N(6)–C(23)	122.8(6)	C(14)–N(6)–Li(2)	105.5(6)
C(14)–N(6)–Li(4)	72.5(5)	C(23)–N(6)–Li(2)	119.5(7)
C(23)–N(6)–Li(4)	90.2(5)	Li(2)–N(6)–Li(4)	70.7(6)
C(27)–N(7)–C(28)	123.6(5)	C(27)–N(7)–Li(5)	84.7(5)
C(27)–N(7)–Li(6)	76.3(4)	C(28)–N(7)–Li(5)	149.0(6)
C(28)–N(7)–Li(6)	90.6(4)	Li(5)–N(7)–Li(6)	83.9(5)
C(27)–N(8)–C(32)	120.0(5)	C(27)–N(8)–Li(5)	71.8(4)
C(27)–N(8)–Li(6)*	107.5(5)	C(32)–N(8)–Li(5)	90.0(4)
C(32)–N(8)–Li(6)*	119.0(5)	Li(5)–N(8)–Li(6)*	69.9(5)
C(27)–N(9)–C(36)	120.3(5)	C(27)–N(9)–Li(5)*	112.7(5)
C(27)–N(9)–Li(6)	81.1(5)	C(36)–N(9)–Li(5)*	91.5(5)
C(36)–N(9)–Li(6)	157.3(5)	Li(5)*–N(9)–Li(6)	71.7(5)
N(1)–C(1)–N(2)	118.8(6)	N(1)–C(1)–N(3)	119.8(6)
N(2)–C(1)–N(3)	120.1(6)	N(1)–C(2)–C(3)	113.6(6)
N(4)–C(14)–N(5)	119.0(6)	N(4)–C(14)–N(6)	118.6(6)
N(5)–C(14)–N(6)	120.8(6)	N(7)–C(27)–N(8)	118.7(5)
N(7)–C(27)–N(9)	119.0(5)	N(8)–C(27)–N(9)	120.3(5)
N(1)–Li(1)–N(2)	68.4(4)	N(1)–Li(1)–N(5)	103.6(6)
N(2)–Li(1)–N(5)	128.5(7)	N(2)–Li(2)–N(3)	67.9(4)
N(2)–Li(2)–N(6)	133.2(9)	N(3)–Li(2)–N(6)	111.8(7)
N(1)–Li(3)–N(4)	132.4(8)	N(1)–Li(3)–N(5)	113.4(6)
N(4)–Li(3)–N(5)	69.7(5)	N(3)–Li(4)–N(4)	129.4(7)
N(3)–Li(4)–N(6)	104.6(6)	N(4)–Li(4)–N(6)	68.2(4)
N(7)–Li(5)–N(8)	68.5(4)	N(7)–Li(5)–N(9)*	132.0(6)
N(8)–Li(5)–N(9)*	101.1(5)	N(7)–Li(6)–N(8)*	132.6(6)
N(7)–Li(6)–N(9)	68.0(4)	N(8)*–Li(6)–N(9)	115.5(6)

[a] Symmetry code for starred atoms: $-x-1$, $-y+1$, $-z+1$.

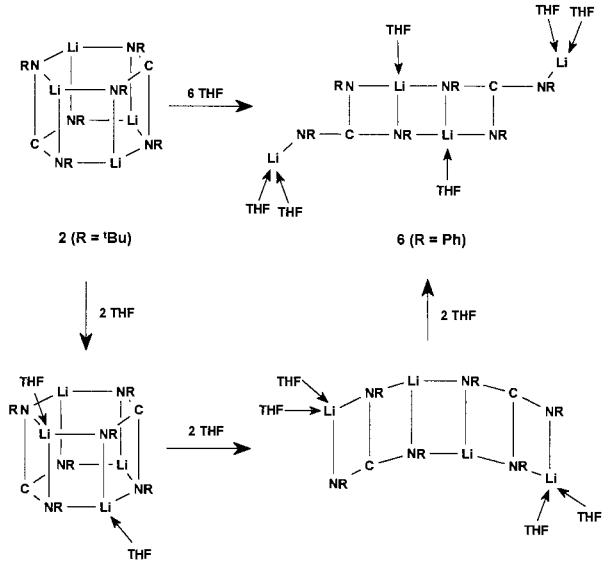

Fig. 5. Schematic representation of the structural relationship between $\{Li_2[C(N^tBu)_3]\}_2$ (**2**) and $\{Li_2[C(NPh)_3]\}_2(THF)_6$ (**6**) [2]. For clarity the structure of **2** is shown as an undistorted hexagonal prism.

two lithium atoms results in the unravelling of the $C_2N_6Li_4$ cage to give the observed structure of $\{Li_2[C(NPh)_3]\}_2(THF)_6$ (**6**) [2]. In addition, the lithium atoms are coordinated to the phenyl groups in $\{Li_2[C(NPh)_3]\}_2(THF)_6$ [2]. A similar 'dis-assembling process' has been proposed in the case of lithium anilide $[(PhNNLi)_6 \cdot 8THF]$ [22].

The centrosymmetric $C_2N_6Li_4$ core (**A** in Fig. 3) has C_i symmetry with crystallographically inequivalent lithium atoms Li(5) and Li(6). However, the ^{7}Li NMR spectrum of **2** in C_7D_8 solution at 25 °C exhibits a singlet at δ −2.37. In addition, a weak singlet at δ −2.52 (ratio ca. 1:6) is observed which may be due to another oligomer of **2**. Three resonances in the ratio of 1:1:1 are expected in the ^{1}H NMR for the inequivalent ^{t}Bu groups. However, the ^{1}H NMR spectrum of **2** in C_6D_6 solution shows only one singlet at δ 1.40 at room temperature (cf. $\delta(^1H)$ 1.17 for $^tBuN{=}C{=}N^tBu$ in C_6D_6 [23]). Thus both the ^{7}Li and ^{1}H NMR data imply a highly fluxional structure for **2**. The related dimers $Li_2[E(N^tBu)_3]\_2$ (E = Se, Te) [5–7] are also stereochemically non-rigid in C_7D_8 solution and the mechanism of this fluxional process has been discussed for $\{Li_2[Te(N(^tBu)_3]\}_2$ [6]. However, the decreasing solubility of **2** with decreasing temperature prevents a detailed analysis of the complex ^{1}H NMR spectra below 267 K. The central carbon of **2** gives rise to a resonance at $\delta(^{13}C)$ 181.7 which is to considerably higher frequency than that in **1** and in $^tBuN{=}C{=}N^tBu$ ($\delta(^{13}C$ in d_8-THF) 139.6) [23]. The ^{13}C chemical shift for the central carbon in $\{Li_2[C(NPh)_3]\}_2(THF)_6$ was observed at δ 169.4 in d_8-THF solution [2].

In summary, we have developed a potentially versatile route to triazatrimethylene methane dianions $C(NR)_3^{2-}$ from carbodiimides. In the specific case of R = ^{t}Bu, the presence of a convenient ^{1}H NMR probe and superior solubility in organic solvents are definite advantages for the development of the ligand chemistry of this dianion and the corresponding monanion $[C(N^tBu)_2(HN^tBu)]^-$.

Acknowledgements

We thank Andrew Downard for helpful discussions. Financial support from the Natural Sciences and Engineering Research Council (NSERC, Canada) is gratefully acknowledged.

References

[1] D.R. Armstrong, D. Barr, W. Clegg, R.E. Mulvey, D. Reed, R. Snaith, K. Wade, J. Chem. Soc. Chem. Commun. (1986) 869.
[2] (a) P.J. Bailey, A.J. Blake, M. Kryszczuk, S. Parsons, D. Reed, J. Chem. Soc. Chem. Commun. (1995) 1647. (b) P.J. Bailey, L.A. Mitchell, P.R. Raithby, M.-A. Rennie, K. Verhorevoort, D.S. Wright, Chem. Commun. (1996) 1351.
[3] M.B. Dinger, W. Henderson, Chem. Commun. (1996) 211.
[4] H. Quast, E. Schmidt, Chem. Ber. 103 (1970) 1249.
[5] T. Chivers, X. Gao, M. Parvez, Angew. Chem. Int. Ed. Engl. 34 (1995) 2549.
[6] T. Chivers, X. Gao, M. Parvez, Inorg. Chem. 35 (1996) 4336.
[7] T. Chivers, M. Parvez, G. Schatte, Inorg. Chem. 35 (1996) 4094.
[8] R. Fleischer, S. Freitag, F. Pauer, D. Stalke, Angew. Chem. Int. Ed. Engl. 35 (1996) 204.
[9] (a) M. Wedler, F. Knösel, M. Noltemeyer, F.T. Edelmann, U. Behrens, J. Organomet. Chem. 388 (1990) 21. (b) J.R. Hagadorn, J. Arnold, Inorg. Chem. 36 (1997) 132. (c) Y. Zhov, D.S. Richeson, Inorg. Chem. 36 (1997) 501.
[10] N.D.R. Barnett, W. Clegg, L. Horsburgh, D.M. Lindsay, Q.-Y. Liu, F.M. Mackenzie, R.E. Mulvey, P.G. Williard, Chem. Commun. (1996) 2321.
[11] D.D. Perrin, W.L.F. Armarego, Purification of Laboratory Chemicals, Pergamon, New York, 3rd edition, 1988.
[12] A. Altomare, M.C. Burla, M. Camalli, M. Cascarano, C. Giacovazzo, A. Guagliardi, G. Polidori, in preparation.
[13] P.T. Beurskens, G. Admiraal, G. Beurskens, W.P. Bosman, R. de Gelder, R. Israel, J.M.M. Smith, The DIRFIX-94 Program System, Technical Report of the Crystallography Laboratory, University of Nijmegen, Netherlands, 1994.
[14] D.T. Cromer, J.T. Waber, International Tables for X-Ray Crystallography, vol. IV, Kynoch Press, Birmingham, UK, 1974, Table 2.2A.
[15] J.A. Ibers, W.C. Hamilton, Acta Crystallogr. 17 (1964) 781.
[16] F. Hai-Fu, SAPI91 Structure Analysis Program with Intelligent Control, Rigaku Corporation, Tokyo, Japan, 1991.
[17] TEXSAN: Crystal Structure Package, Molecular Structure Corporation, 1985, 1992.
[18] T. Chivers, X. Gao, M. Parvez, Inorg. Chem. 35 (1996) 553.
[19] F.H. Allen, O. Kennard, D.G. Watson, L. Brammer, A.G. Orpen, R. Taylor, J. Chem. Soc. Perkin Trans. II: (1987) S1.
[20] D. Stalke, M. Wedler, F.T. Edelmann, J. Organomet. Chem. 431 (1992) C1.
[21] R.E. Mulvey, Chem. Soc. Rev. 20 (1991) 167.
[22] W. Clegg, L. Horsburgh, F.M. Mackenzie, R.E. Mulvey, J. Chem. Soc. Chem. Commun. (1995) 2011.
[23] T. Chivers, G. Schatte, unpublished results.